Precise Test of Electroweak Theory from a New Measurement of Parity Nonconservation in Atomic Thallium

P. A. Vetter, D. M. Meekhof,* P. K. Majumder,† S. K. Lamoreaux, and E. N. Fortson
Department of Physics, FM-15, University of Washington, Seattle, Washington 98195
(Received 2 November 1994)

We report a new measurement of parity nonconserving (PNC) optical rotation near the 1.28 μm, $6P_{1/2} \rightarrow 6P_{3/2}$ magnetic dipole transition in thallium. We find the ratio of the PNC $E1$ amplitude to the $M1$ amplitude to be $\mathcal{R} = (-14.68 \pm 0.17) \times 10^{-8}$, which within the present uncertainty of atomic theory yields the thallium weak charge $Q_w(^{205}\mathrm{Tl}) = -114.2 \pm 3.8$ and the electroweak parameter $S = -2.2 \pm 3.0$. Separate measurements on the $F = 1$ and $F = 0$ ground-state hyperfine components of the transition yield $\mathcal{R}_1 - \mathcal{R}_0 = (0.15 \pm 0.20) \times 10^{-8}$, which limits the size of nuclear spin-dependent PNC in Tl.

PACS numbers: 32.80.Ys, 11.30.Er

The electroweak standard model predicts parity nonconservation (PNC) in atoms caused (in lowest order) by exchange of the Z_0 boson between atomic electrons and quarks in the nucleus [1]. Single-isotope measurements of atomic PNC are sensitive to isospin-conserving electroweak radiative corrections and to the possible existence of a second Z_0 boson [2]. PNC has been measured to a precision of 1% in lead [3], and to 2% in cesium [4] and bismuth [5], but the interpretation of these experiments in terms of electroweak physics requires accurate atomic calculations as well. In the case of cesium, PNC has been calculated to an accuracy of 1% [6], and for a number of years this element has provided the sole atomic test of the standard model.

We report here the results of a 1% measurement of PNC optical rotation on the 1.283 μm, $6P_{1/2} \rightarrow 6P_{3/2}$ $M1$ line of thallium. Combined with the existing 3% calculation of PNC for this line [7], our measurement provides a new atomic test of the standard model comparable in overall accuracy to cesium, with the potential for further improvement in new thallium calculations now underway [8,9]. Previous measurements of PNC in thallium [10], including a measurement of optical rotation on the 1.283 μm line [11], achieved a 15% level of accuracy.

The two naturally occurring isotopes of thallium (^{205}Tl and ^{203}Tl) have nuclear spin ($I = 1/2$) and large ground-state hyperfine splitting (21.3 GHz). By separately measuring the amplitude of PNC on the two well-resolved hyperfine lines (henceforth called $F \equiv F_g = 0, 1$), we can search for the much smaller nuclear spin-dependent (SD) PNC effects, principally caused in Tl by the nuclear anapole moment [12]. Experimental evidence of nuclear spin-dependent PNC effects has been reported, in cesium, at about 2σ resolution [4].

For comparison with electroweak theory, the nuclear spin-independent (SI) quantity of interest in all atomic PNC experiments is the so-called weak charge, $Q_w(Z,N)$, which in the standard model at tree level is $Q_w = -N + Z(1 - 4\sin^2\theta_w)$, where θ_w is the weak mixing angle. Radiative corrections within the standard model change Q_w at the several percent level [13]. Corrections due to heavy physics (Higgs boson and top quark) and to unknown particles can be divided into isospin-conserving and isospin-breaking components, labeled S and T, respectively. Atomic PNC is unique among electroweak physics tests in that the T dependence in Q_w nearly cancels for values of Z/N characteristic of heavy atoms [2,13,14]. Including radiative corrections yields, to a good approximation,

$$Q_w(^{205}\mathrm{Tl}) = -116.8 - 1.2\mathbf{S} + Q_{\mathrm{new}}^{\mathrm{tree}}, \qquad (1)$$

where S is defined as in [2], and the final term accounts for new tree-level physics such as a second Z_0 boson.

We measure $\mathcal{R} \equiv \mathrm{Im}(\mathcal{E}_{\mathrm{PNC}}/\mathcal{M})$, where $\mathcal{M}$ is the magnetic dipole amplitude, and $\mathcal{E}_{\mathrm{PNC}}$ is the electric dipole amplitude which connects the ground and excited P states only through the weak interaction parity admixture. We express $\mathcal{R}$ for a given ground-state hyperfine line as

$$\mathcal{R}(F) = C(Z)[Q_w(Z,N) + 4\kappa_a\xi(F)]. \qquad (2)$$

$C(Z)$ contains effects of atomic structure and must be calculated by many-electron atomic theory. The second term inside the brackets contains all SD effects and is expected to be small ($\approx$1), with $\xi(0) = 1$ and $\xi(1) = -1/3$ in the single-electron approximation [15]. If the anapole contribution dominates, κ_a is then the nuclear anapole moment defined in [12]. We see from Eq. (2) that PNC must be measured on both hyperfine lines to determine the SD and SI components of $\mathcal{R}$, the former resulting from a difference measurement and the latter from a weighted average. If we define $\mathcal{R}_1$ ($\mathcal{R}_0$) as the PNC measurement for ground-state $F = 1$ (0) then the nuclear spin-independent component of $\mathcal{R}$ is found by computing $\mathcal{R}_{\mathrm{SI}} \equiv C(Z)\,Q_w = \frac{3}{4}\mathcal{R}_1 + \frac{1}{4}\mathcal{R}_0$. We also define $\Delta\mathcal{R}_{\mathrm{SD}} \equiv \mathcal{R}_1 - \mathcal{R}_0 \approx 0.046\,\kappa_a\mathcal{R}_{\mathrm{SI}}$. We have separately analyzed the data from each hyperfine line to deduce results for $\mathcal{R}_{\mathrm{SI}}$ and $\Delta\mathcal{R}_{\mathrm{SD}}$.

 0031-9007/95/74(14)/2658(4)$06.00

We measure PNC by the rotation of the plane of polarization of a laser beam produced by passage through a column of thallium vapor. The PNC optical rotation angle is $\phi_P(\nu) = -4\pi L\nu c^{-1}[n(\nu) - 1]\mathcal{R}$, where ν is the optical frequency, $n(\nu)$ is the refractive index due to the absorption line, and L is the path length. Because $n(\nu)$ follows a dispersion curve, the characteristic shape of $\phi_P(\nu)$ across the absorption line discriminates against contamination from other rotations.

Our experiment was performed with the same apparatus used for our recent 1% measurement on the 1.279 μm $M1$ line in lead [3], and we describe the apparatus only briefly here. Light from an external cavity InGaAs diode laser at 1.283 μm passes through a polarizing calcite prism, a Faraday rotator, a 1 m length of thallium vapor, and an analyzing prism, and then enters an InGaAs p-i-n photodiode detector. Some of the laser output is sent through a Fabry-Pérot cavity to measure the laser frequency as we scan it across the transition. The thallium vapor is produced in an oven heated to 850–1100 °C, and is confined by a 10–50 torr buffer gas of helium plus 5% hydrogen (to prevent oxidation of the sample). The calcite prisms and oven chamber windows produce spurious wavelength-dependent optical rotations of order 10^{-6} rad. We measure this background and subtract it from the thallium optical rotation data by moving an empty dummy tube into the optical path (leaving all optics undisturbed) and scanning the laser frequency to obtain background rotation data.

We have taken 62 days of data (about 2600 thallium/dummy tube cycles in 500 h) at optical depths from 3 to 70 absorption lengths (measured at the wavelength of peak absorption) while scanning the laser across either the $F = 0$ or 1 hyperfine group. We have also taken 14 days of data during which we scanned the laser continuously across both hyperfine groups.

Each measurement cycle is analyzed by performing nonlinear least-square fits of the line-shape data. The theoretical profiles for the transmission, Faraday, and PNC line shapes consist of Doppler and Lorentz-broadened Voigt profiles summed over the different isotopic and hyperfine lines. (These include the small electric quadrupole component of the transition, which does not interfere with $\mathcal{E}_{\mathrm{PNC}}$ to produce PNC rotation, but does affect the Faraday and absorption line shapes. We measure $\mathcal{E}_2/\mathcal{M} = 0.240 \pm 0.002$, with the uncertainty producing negligible error in either $\mathcal{R}_0$ or $\mathcal{R}_1$.) The transmission data are fit to find line-shape parameters including the two widths, the optical depth, and the intensity of nonresonant laser light (<0.1% of the intensity in the main mode with no observable spectral features). We use these parameters to generate a Faraday rotation line shape from which we extract a fitted amplitude of the Faraday rotation data. For a known magnetic field and optical depth, this calibrates the PNC measurement. The quality of these fits can be seen in Fig. 1. Finally, the PNC angle data minus the empty tube

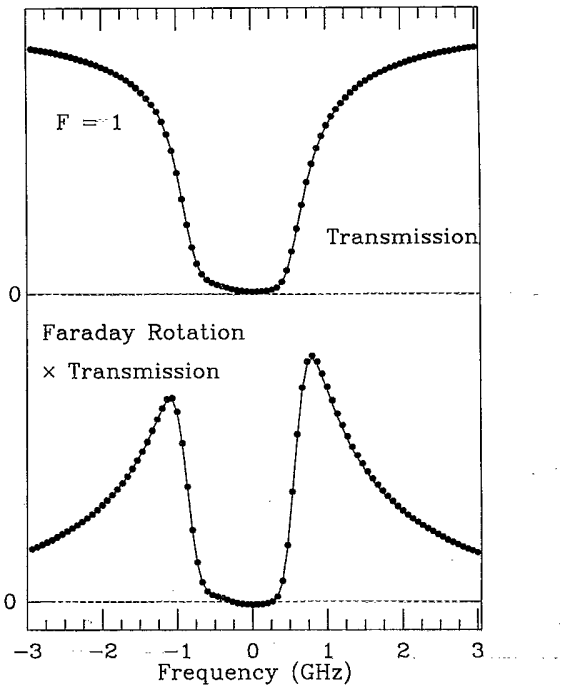

FIG. 1. Transmission and Faraday rotation data (points) and fits (solid lines) from all data cycles on $F = 1$ binned together.

angle data are fit by $I(\nu)[\phi_F(\nu) + \phi_P(\nu) + \Delta\phi_B(\nu)]$. The transmitted resonant laser light $I(\nu)$ is a known function from the transmission line-shape fit. The remaining background rotation which is not successfully subtracted out due to drifting or other effects is denoted here by $\Delta\phi_B(\nu)$. Inclusion of $\phi_F(\nu)$ allows for Faraday rotation from residual magnetic field (typically 0.2 mG, causing rotation of order 1 μrad). The residual field is reset after each run, and we observe no correlation of $\mathcal{R}_0$ or $\mathcal{R}_1$ with this field. Higher order effects, such as nonlinear Faraday rotation and dichroism due to transverse fields, are too small to be included, and are strongly rejected by the symmetry of the PNC line shape and averaging over polarizer orientations. Figure 2 shows the combined averaged PNC rotation data and theoretical line shape for all the data accumulated for the $F = 1$ transition.

An independent mechanical calibration is performed by measuring the response to a physical rotation of the polarizers—this is uncertain at 0.7% due to polarizer imperfections and laser beam divergence. The Faraday and mechanical calibrations agree on both hyperfine groups within this uncertainty. Since many uncertainties, such as in mechanical calibration and optical depth, cancel in the ratio of the PNC fit by the Faraday fit, we use the atomic Faraday calibration for the final values of $\mathcal{R}_{\mathrm{SI}}$ and $\mathcal{R}_{\mathrm{SD}}$, but we also produce values with the mechanical calibration to check for error in this procedure.

The statistical uncertainty in $\mathcal{R}$ is due partly to detector (Johnson) noise and photon shot noise but mainly to fluctuations in the unsubtracted background pattern $\Delta\phi_B(\nu)$ in

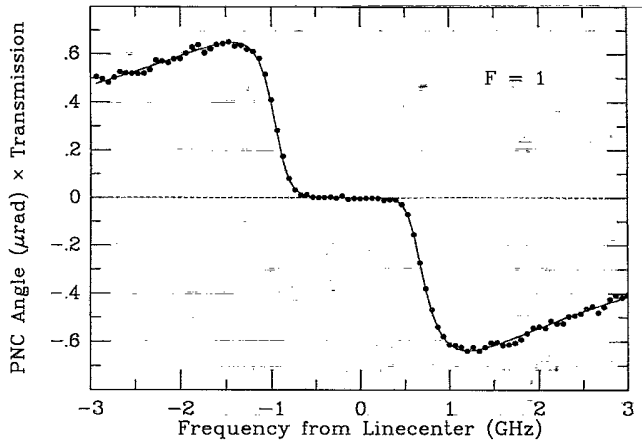

FIG. 2. Combined PNC optical rotation for all data cycles (about 230 h) for $F = 1$ (points) and theoretical (dispersion × transmission) line shape (solid line).

the PNC rotation data. In each data cycle, $\Delta\phi_B(\nu)$ has some random projection on the dispersive PNC profile and contributes an error to the fit. $\Delta\phi_B(\nu)$ is sensitive to optical alignment and other conditions, and changes from cycle to cycle, leading to a scatter of the PNC fits, and values of $\mathcal{R}$. Although $\Delta\phi_B(\nu)$ has some variation slower than the data cycle period, causing the day-to-day scatter of $\mathcal{R}$ to be larger than what the cycle-to-cycle scatter would imply ($\chi^2 \sim 2.6$), we observe no evidence of persistent features in $\Delta\phi_B(\nu)$ over time scales longer than 1 day. The scatter of $\mathcal{R}$ between groups of days agrees with the daily scatter within each group, with $\chi^2 \approx 1$. The daily statistical precision in the value of $\mathcal{R}$ is roughly 10% at the lowest optical depths and about 1% at the highest optical depths where the PNC signal is much larger. We have taken more data at the lower optical depths to give them comparable statistical power to that of the higher depths. The final statistical error in the data comes from the scatter among the statistically independent daily averages of $\mathcal{R}$.

We have made an extensive study of possible systematic errors. The most important class of errors involves systematic differences between the theoretical line-shape profiles and the shapes we observe. The Voigt line shapes assumed in the analysis do not allow for non-Lorentz collisional broadening, for vapor density variations along the optical path or in time, or for instrumental effects such as laser line shapes. As a result, residual features of order 0.1% appear in the difference between the absorption data and the fitted theoretical absorption profile, and somewhat larger residuals appear in the fitted Faraday data (with an rms deviation from zero about 0.2%–1.0% of the rms signal size on $F = 1$). When all of the PNC optical rotation data are combined, we observe line-shape residuals no larger than 1.0% and dominated by noise.

To place limits on the uncertainties in $\mathcal{R}$ associated with these line-shape misfits, we compared the values of $\mathcal{R}$ for several fitting procedures applied on all data, for data at different optical depths, and for the two sweep directions (increasing and decreasing laser frequency). Table I lists the results (weighted averages of all days of data) of a number of these different fitting procedures, which emphasize different portions of the line profile where residual misfits are different, and includes in one case a modeling of $\Delta\phi_B(\nu)$ with terms linear and quadratic in ν in addition to the usual dc offset angle. The five analyses yield the same value of $\mathcal{R}$ within the statistical uncertainties of a few tenths of 1%. The agreement between points in the line wings and near the line center is particularly significant since these points do not overlap at all. Results using the mechanical calibration on the same data are also in Table I, as well as the results from the wide laser sweep data, both of which are consistent with the other analyses. Figure 3 shows the values of $\mathcal{R}$ plotted versus optical depth for data sets taken at different Tl vapor densities. There are major changes in line shape and in sensitivity to background over the full range in optical depth (a factor of 5) represented here. The data sets at the different optical depths agree quite well within statistical error bars.

To allow for any possible correlation of $\mathcal{R}$ with optical depth we assign a component of systematic error in $\mathcal{R}$ equal to the observed range of variation in $\mathcal{R}$ over all optical depths, to which we add an uncertainty for similar maximum variations between up and down sweeps and among the different fitting procedures, yielding a combined line-shape systematic error of 1.0%, which is consistent as well with the size of the residual misfits in the data. Including a 0.3% uncertainty in the magnetic field applied for the Faraday calibration, we obtain a total systematic error of 1.1%.

We take an average of the values in Table I deriving from the several fit methods with atomic Faraday calibration to obtain our final value of the nuclear spin-independent PNC optical rotation (normalized to ^{205}Tl),

$$\mathcal{R}_{\mathrm{SI}}(^{205}\mathrm{Tl}) = (-14.68 \pm 0.06 \pm 0.16) \times 10^{-8}, \quad (3)$$

with statistical and systematic errors, respectively. We also present a result extracted by using the mechanical calibration alone, which is still susceptible to line-shape error in the transmission and parity line-shape fits, but not

TABLE I. Results for $\mathcal{R}$ in units of 10^{-8} from different line-shape fitting methods.

Fit method	$\mathcal{R}_0$	$\mathcal{R}_1$	$\Delta\mathcal{R}_{\mathrm{SD}}$
Lin + quad terms	−15.02(11)	−14.70(05)	+0.30(12)
(Noise)$^{-2}$ weight	−14.75(12)	−14.66(06)	+0.07(13)
Flat weight	−14.58(12)	−14.53(06)	−0.08(17)
Line wings only	−14.67(19)	−14.53(09)	+0.07(22)
Near line center	−14.83(13)	−14.63(05)	+0.21(13)
Mechanical calib.	−14.78(13)	−14.69(06)	0.00(13)
0, 1 in same sweep	−14.88(14)	−14.71(09)	+0.16(17)

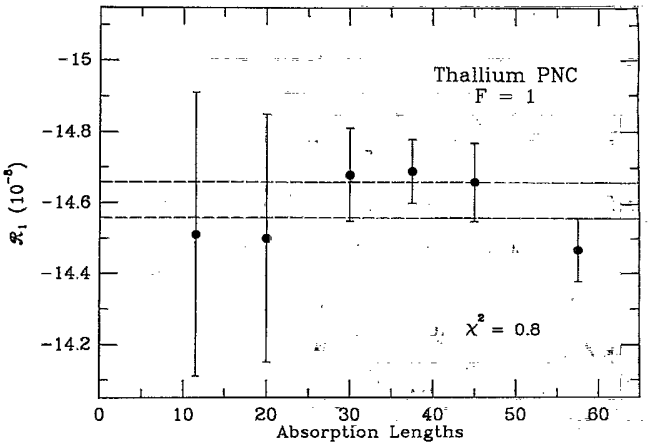

FIG. 3. The value of $\mathcal{R}_1$ plotted versus optical depth for data sets taken at different vapor densities. Error bars show statistical uncertainties only. The horizontal dashed lines represent $\pm 1\sigma$ uncertainty of the combined weighted average of the data sets. The central value for $\mathcal{R}_1$ agrees with the central value extracted from Table I.

the Faraday effect fits. Using the mechanical calibration method, we find $\mathcal{R} = (-14.71 \pm 0.06 \pm 0.20) \times 10^{-8}$, which agrees quite well with the above value.

The calculated PNC-induced $E1$ amplitude [7] for this 1.283 μm transition in ^{205}Tl can be combined with a recent calculated value for the $M1$ matrix element [8] to yield the atomic structure factor $C(\mathrm{Tl}) = (1.29 \pm 0.04) \times 10^{-9}$, where the uncertainty is that quoted for the $E1$ calculation. Using this factor in Eq. (2), with our result for $\mathcal{R}_{\mathrm{SI}}$, we find

$$Q_w(^{205}\mathrm{Tl}) = -114.2 \pm 1.3 \pm 3.4, \quad (4)$$

where the first error is experimental and the second is due to atomic theory. We conclude from Eq. (1) that $S = -2.2 \pm 3.0$, which agrees with existing electroweak tests [16], including the atomic cesium result $S = -2.8 \pm 2.2$ [13], yet would enjoy greatly enhanced significance upon the improvement of the atomic structure calculation.

For the nuclear spin-dependent component of the PNC, using the difference between $\mathcal{R}_1$ and $\mathcal{R}_0$ extracted for each day as well as the data taken over both groups simultaneously, we make a similar analysis of statistical and systematic errors as for $\mathcal{R}_{\mathrm{SI}}$ to obtain our result

$$\Delta\mathcal{R}_{\mathrm{SD}} = (0.15 \pm 0.13 \pm 0.15) \times 10^{-8}. \quad (5)$$

As a check, if we extract $\Delta\mathcal{R}_{\mathrm{SD}}$ using the mechanical calibration we find $\Delta\mathcal{R}_{\mathrm{SD}} = (0.00 \pm 0.13 \pm 0.31) \times 10^{-8}$. Within the independent particle, single-electron approximation, our result for $\Delta\mathcal{R}_{\mathrm{SD}}$ yields the value

$$\kappa_a = -0.22 \pm 0.30, \quad (6)$$

for the nuclear anapole moment of thallium, compared with theoretical values [17] which are centered around $\kappa_a = +0.40$ with consistency at about the 15% level.

This work is supported by National Science Foundation Grant No. PHY-9206408.

*Present address: Time and Frequency Division, National Institute of Standards and Technology, Boulder, CO 80303.

†Present address: Department of Physics, Williams College, Williamstown, MA 01267.

[1] M. A. Bouchiat and C. C. Bouchiat, Phys. Lett. **48B**, 111 (1974).

[2] M. E. Peskin and T. Takeuchi, Phys. Rev. D **46**, 381 (1992).

[3] D. M. Meekhof *et al.*, Phys. Rev. Lett. **71**, 3442 (1993). We expect to publish a longer explication in which we discuss some experimental details and sytematic effects in fuller detail.

[4] M. C. Noecker, B. P. Masterson, and C. E. Wieman, Phys. Rev. Lett. **61**, 310 (1988).

[5] M. J. D. Macpherson *et al.*, Phys. Rev. Lett. **67**, 2784 (1991).

[6] S. A. Blundell, J. Sapirstein, and W. R. Johnson, Phys. Rev. D **45**, 1602 (1992); V. A. Dzuba *et al.*, Phys. Lett. A **141**, 147 (1989).

[7] V. A. Dzuba *et al.*, J. Phys. B **20**, 3297 (1987).

[8] A. M. Martensson-Pendrill, also a calculation of the $E2$ amplitude (private communication).

[9] W. R. Johnson, J. Sapirstein, and Z. W. Liu (private communication).

[10] P. S. Drell and E. D. Commins, Phys. Rev. A **32**, 2196 (1985).

[11] T. D. Wolfenden, P. E. G. Baird, and P. G. H. Sandars, Europhys. Lett. **15**, 731 (1991).

[12] V. V. Flambaum and I. B. Khriplovich, Zh. Eksp. Teor. Fiz. **79**, 1656 (1980) [JETP **52**, 835 (1980)]; V. V. Flambaum, I. B. Khriplovich, and O. P. Sushkov, Phys. Lett. **146B**, 367 (1984); cf. C. Bouchiat and C. A. Piketty, Z. Phys. C **49**, 91 (1991).

[13] B. W. Lynn, P. G. H. Sandars, J. Phys. B **27**, 1469 (1994).

[14] W. J. Marciano and J. L. Rosner, Phys. Rev. Lett. **65**, 2963 (1990).

[15] I. B. Khriplovich, Budker Institute of Nuclear Physics, Report No. BINP 94–56, 1994 (unpublished). Many-electron theory is also being applied to the spin-dependent term: B. Das and A. Singh (private communication).

[16] C. P. Burgess *et al.*, Phys. Lett. B **326**, 276 (1994).

[17] V. F. Dmitriev, I. B. Khriplovich, and V. B. Telitsin, Nucl. Phys. **A577**, 691 (1994); C. Bouchiat and C. A. Piketty, Phys. Lett. B **269**, 195 (1991).